

RESEARCH ARTICLE



Quantum-Based Optical Pulse Control and Phase Shifts in Chiral Media for IoT Applications

Saddam Hussain and Syed Sajid Ullah 2,3,*

- ¹School of Digital Science, Universiti Brunei Darussalam, Jalan Tungku Link, Gadong, BE1410, Brunei Darussalam
- ² Department of Information and Communications Technology, University of Agder, 4898 Grimstad, Norway

Abstract

Quantum-based models are used to improve the Internet of Things (IoT) ecosystems' efficiency, storage capacity, processing speed, and security. These models investigate quantum effects such as subluminality/superluminality, time delay, and phase shifting to achieve the mentioned goals. Mostly, these models use achiral atomic media that deal with the light beam in a straight path and fail to provide the most needed properties of efficient decision-making, optical routing, control of polarization, and enhanced security. In order to make up for these deficiencies, an investigation into the propagation of a light beam through a chiral atomic medium has been carried out. decision-making and optical routing system that is efficient for quantum-based IoT devices is provided by the light beam being split into left and right circularly polarized light. The maximum possible values of the group indices are scaled up to $n(pm)_q =$ pm1000 in this exercise. This is equivalent to having group velocities of $v(pm)_q = pmc/1000$. The Left-Handed Circularly Polarized Light (LCP)

Submitted: 16 July 2025 **Accepted:** 28 July 2025 **Published:** 22 August 2025

Vol. 1, **No.** 1, 2025. **10**.62762/JQC.2025.506482

 and Right-Handed Circularly Polarized Light (RCP) beams show subluminal propagation when the value of group velocity $v(pm)_g = +c/1000$ is positive, while the value of velocity $v(pm)_g = -c/1000$ indicates superluminal propagation, which increases the data transfer speed in the IoT. The maximum phase shifts in RCP and LCP beams are measured to $\pm 10^5$ Micro-radian and group phase shifts are measured to $\pm 10^5$ micro-radian, used to enhance the security of IoT as well as minimize losses. In the chiral medium, the highest fractional change that can be detected in group indices, group delay time, and group phase shifts of LCP and RCP beams is pm10 = pm1000.

Keywords: quantum computing, chiral medium, internet of things, quantum effects.

1 Introduction

Recently, quantum—based technological innovations have been used to improve the speed, efficiency, storage capacity, and security of the IoT ecosystems [1, 2]. Many techniques, such as manipulation of group velocity, time delay, and phase shifting, are used to achieve the proposed goals. The mentioned techniques use electromagnetic waves (EM-waves) within the

Citation

Hussain, S., & Ullah, S. S. (2025). Quantum-Based Optical Pulse Control and Phase Shifts in Chiral Media for IoT Applications. *Journal of Quantum Cryptography*, 1(1), 5–13.



© 2025 by the Authors. Published by Institute of Central Computation and Knowledge. This is an open access article under the CC BY license (https://creativecommons.org/licenses/by/4.0/).

³Center for Cybersecurity Cluster, School of Computer Science, The University of Sydney, Sydney, Australia

atomic medium [3].

The group velocity of EM waves gives rise to the subluminal and superluminal effects for enhancing data transfer speed in IoT. These effects are achieved in an atomic medium by controlling the group index [4]. The positive value of the group index corresponds to the subluminal effect, while its negative value is related to the superluminal effect. In the superluminal case, the data transfer is faster than the conventional one [5]. The delay time quantum technique is used to increase small IoT devices' storage capacity. In an atomic medium, it is investigated through the group index. The decrease in delay time to a negative value increases the amount of data that can be stored in small IoT devices. The phase shifting technique is used to secure the transmission and minimize losses of critical IoT data. In phase shifting, the information packets are further divided into sub-parts. A phase difference is then measured between them. This effect enhances quantum cryptographic techniques to improve IoT security [6].

Recently, Karim et al. [6] presented a quantum-based model to investigate the subluminal/superluminal effects, delay time, and phase shift, with some impressive results. They also provided the deployment of these techniques in IoT. The authors used a normal (achiral) atomic medium. Achiral medium lacks the important properties of efficient decision-making, optical routing, control of polarization, and enhanced security. On the other hand, a chiral medium solves the above-mentioned shortcomings. A chiral medium splits a light beam into two parts, i.e., LCP and RCP [7]. This property enhances the decision-making ability of quantum sensors. Further, it is used in cutting-edge artificial intelligence (AI). Moreover, chiral media can manipulate the polarization state of light passing through them [8]. This phenomenon enables efficient optical routing, where EM waves are diverted from faulty routers to functional ones. It also results in enhanced phase shifting, providing strength to IoT security.

1.1 Motivation and contributions

Given the above discussions, we proposed an improved quantum-based model for IoT ecosystems using spherical manipulation of optical pulses and giant phase shifts in a chiral medium. By introducing the chiral atomic medium, we investigated the subluminal/superluminal effects, time delay, and phase shifting. The main contributions of the proposed advanced model are given below.

- In the present study, we used a chiral atomic medium with four levels and both electric and magnetic fields. LCP and RCP light is created when the light beam is divided, which enables efficient decision-making and optical routing for quantum-based Internet of Things devices.
- For both LCP and RCP beams, the group index is quantified to an accuracy of ± 1000 .
- The group velocity of $\pm c/1000$ is achieved, whose negative value gives rise to the superluminal effect that enhances the data transmission speed in IoT.
- The maximum phase shift in LCP and RCP, as well as a group phase shift of 10⁵ micro – radian is obtained and used to improve the security of IoT.
- The measurement involves quantifying the fractional change in group indices, delay time, and group phase shift within a range of approximately $\pm 10 = 1000\%$.
- In the end, we provide a use case for the proposed model in IoT.

1.2 Paper organization

The paper is organized as section 2, which consists of the outlines of our proposed network and atomic models and the methodology. In section 3, the results of our study are presented. The deployment of our proposed schemes in IoT is presented in section 4 and, finally, in section 5, the summarization and conclusion of our findings are given.

2 Models and Its Dynamics

In the current section, the IoT and atomic models are provided.

2.1 Proposed model for IoT devices

In Figure 1, we show the proposed network model for quantum-based IoT. The participants and their roles are given below.

- 1. **IoT and Sensors:** These devices transmit data based on quantum techniques.
- 2. **Security provider:** A trusted third party that provides and manages the security of an IoT network.
- 3. **Proposed chiral atomic medium:** This medium can split the light beam into LCP and RCP, enabling effective decision-making and enhanced security of IoT.



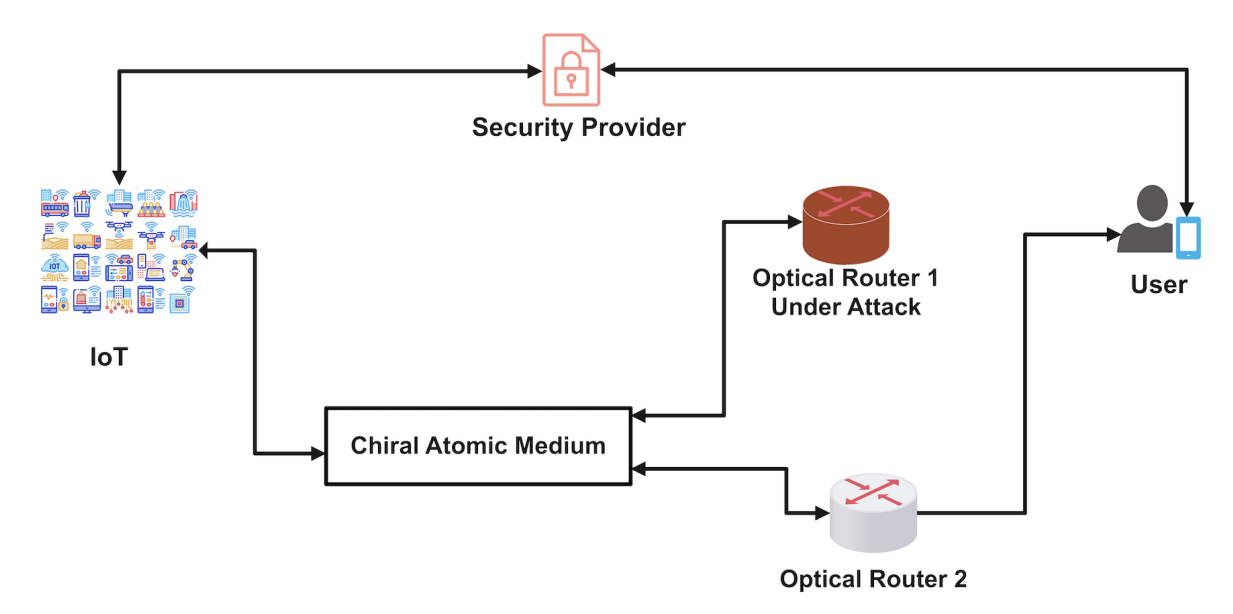


Figure 1. Model for IoT devices.

- 4. **Optical routers:** These are categorized as router 1 (faulty one) and router 2 (functional one). The work of these routers is based on the proposed chiral atomic medium.
- 5. **Users:** The users include persons, devices, and systems that receive the transmitted data from IoT and sensors.

2.2 Proposed System Model

This study examines a Chiral atomic medium consisting of four levels. The objective is to investigate the influence of this medium on the absorption, refractive/group indices, and phase shifts for the LCP and RCP, as depicted in Figure 2. In the present system, the electric probe field denoted as E_p is characterized by its Rabi frequency Λ_p and detuning Δ_p . This field is coupled between the states $|2\rangle$ and $|4\rangle$. The quantum states $|1\rangle$ and $|3\rangle$ are subjected to coupling with a magnetic field denoted as E_m . This magnetic field has a Rabi frequency denoted as Λ_m and a detuning denoted as Δ_m . The states $|3\rangle$ and $|4\rangle$ are connected by the interaction with a control field E_c , which has a Rabi frequency Λ_c and a detuning Δ_c . The states $|1\rangle$ and $|2\rangle$ are originally prepared in a linear superposition described by the state $|\Phi\rangle = \sqrt{x}|2\rangle + \sqrt{1 - x}e^{i\varphi}|1\rangle$, where x and φ are real numbers.

The proposed atomic model's self-Hamiltonian is written as:

$$H_0 = \sum_{i=1}^{4} \hbar \omega_i |i\rangle \langle i| \tag{1}$$

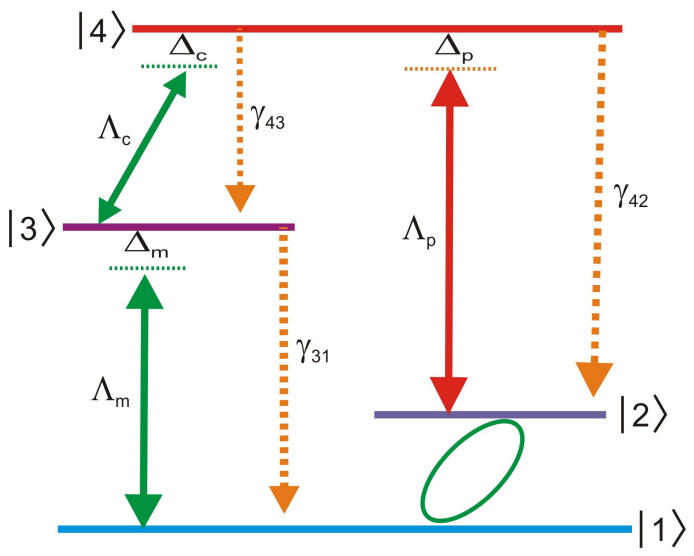


Figure 2. Proposed atomic model.

The system's interaction-Hamiltonian is written by [9]:

$$H_{I} = -\frac{h}{4\pi} \left[\Lambda_{p} e^{-i\Delta_{p}t} \left| 2 \right\rangle \left\langle 4 \right| + \Lambda_{c} e^{-i\Delta_{c}t} \left| 3 \right\rangle \left\langle 4 \right| + \Lambda_{m} e^{-i\Delta_{m}t} \left| 1 \right\rangle \left\langle 3 \right| \right] + \text{H.C.}$$

In the aforementioned equation, $\Lambda_p=\mu_{24}.E_0/\hbar$, while $\Lambda_m=\mu_{13}.B_0/\hbar$. Here, μ_{13} is the magnetic dipole moment between states $|1\rangle$ and $|3\rangle$, while μ_{24} is the electric dipole moment between states $|2\rangle$ and $|4\rangle$. The dipole moments can be mathematically linked to the atomic decays between corresponding states. Specifically, the relationship is expressed as follows: $\mu_{13}=\sqrt{3c^2\hbar\lambda^3\gamma_{31}/8\pi^2}$ and $\mu_{24}=\sqrt{3\hbar\lambda^3\gamma_{42}/8\pi^2}$. The

equation utilized for the temporal evolution of the density matrix, commonly referred to as the master equation [10], is expressed as follows:

$$\begin{split} \frac{\partial \rho}{\partial t} &= -\frac{i}{\hbar} [H_i, \rho] \\ &- \sum \frac{1}{2} \gamma_{ji} \left(R_{ji}^{\dagger} R_{ij} \rho + \rho R_{ji}^{\dagger} R_{ij} - 2 R_{ij} \rho R_{ji}^{\dagger} \right) \end{split}$$

where R_{ji}^{\dagger} is the increasing operator for γ_{ji} atomic decays and R_{ij} is the decreasing operator. The following four electric/magnetic coupled-rate equations are derived by applying the aforementioned master equation to our suggested system.

$$\frac{\partial \widetilde{\rho}_{13}}{\partial t} = \left[i\Delta_m - \frac{1}{2} (\gamma_{43} + \gamma_{31}) \right] \widetilde{\rho}_{13} + \frac{i}{2} \Lambda_m (\widetilde{\rho}_{33} - \widetilde{\rho}_{11}) - \frac{i}{2} \Lambda_c^* \widetilde{\rho}_{14}$$

$$\begin{split} \frac{\partial \widetilde{\rho}_{14}}{\partial t} &= \left[i (\Delta_m + \Delta_c) - \frac{1}{2} \gamma_{31} \right] \widetilde{\rho}_{14} \\ &+ \frac{i}{2} \Lambda_m \widetilde{\rho}_{34} - \frac{i}{2} \Lambda_c \widetilde{\rho}_{13} - \frac{i}{2} \Lambda_p \widetilde{\rho}_{12} \end{split}$$

$$\frac{\partial \widetilde{\rho}_{24}}{\partial t} = [i\Delta_p - \frac{1}{2}\gamma_{42}]\widetilde{\rho}_{24} - \frac{i}{2}\Lambda_c\widetilde{\rho}_{23} + \frac{i}{2}\Lambda_p(\widetilde{\rho}_{22} - \widetilde{\rho}_{44})$$

$$\begin{split} \frac{\partial \widetilde{\rho}_{23}}{\partial t} &= \left[i(\Delta_p - \Delta_c) - \frac{1}{2} (\gamma_{42} + \gamma_{43}) \right] \widetilde{\rho}_{23} \\ &+ \frac{i}{2} \Lambda_p \widetilde{\rho}_{43} + \frac{i}{2} \Lambda_m \widetilde{\rho}_{21} - \frac{i}{2} \Lambda_c^* \widetilde{\rho}_{24} \end{split}$$

In the case of weak probe electric and magnetic fields, where the ratio of the probe wavelength to the characteristic wavelength is much smaller than one (i.e., $\Lambda_{m,p} << \Lambda_c$), the zeroth order terms $\widetilde{\rho}_{11}^{(0)}$, $\widetilde{\rho}_{22}^{(0)}$, $\widetilde{\rho}_{12}^{(0)}$. The quantity $\widetilde{\rho}_{21}^{(0)}$ becomes negligible as a result of the presence of small Rabi oscillations. In the first-order approximation, the density matrix is denoted as $\widetilde{\rho}$ and is equal to the $|\psi\rangle$ and $\langle\psi|$. The calculation of the density matrix involves the superposition of the states.

$$\begin{split} &\widetilde{\rho}_{11}^{(0)} = 1 - x, \\ &\widetilde{\rho}_{22}^{(0)} = x, \\ &\widetilde{\rho}_{12}^{(0)} = \sqrt{x(1-x)} \, e^{i\varphi}, \\ &\widetilde{\rho}_{21}^{(0)} = \sqrt{x(1-x)} \, e^{-i\varphi} \end{split}$$

The magnetization and electric polarization are further related to coherence terms in a chiral atomic medium as: $P = N\mu_{24}\widetilde{\rho}_{42}^{(1)}$ and $M = N\mu_{13}\widetilde{\rho}_{31}^{(1)}$ where N is the number of atoms. Plugging the values of coherence $\widetilde{\rho}_{13}^{(1)}$ and $\widetilde{\rho}_{24}^{(1)}$, the electric polarization and magnetization are modified to the forms: $P = \alpha_{EB}B_0 + \alpha_{EE}E_0$ and $M = \alpha_{BB}B_0 + \alpha_{BE}E_0$, whereas,

$$\alpha_{EE} = \frac{N\mu_{24}^2}{\hbar K_e} \tilde{\rho}_{22}^{(0)} \tag{2}$$

$$\alpha_{BB} = \frac{N\mu_{13}^2}{\hbar K_b} \tilde{\rho}_{11}^{(0)} \tag{3}$$

$$\alpha_{BE} = \frac{N\mu_{13}\mu_{24} \exp\left[i(\varphi_{1} - \varphi_{2})\right] \Lambda_{c} \exp\left[-i(\varphi_{c} + \varphi)\right] \widetilde{\rho}_{21}^{(0)}}{2\hbar K_{b} \left(\Delta_{p} - i(\gamma_{42} + \gamma_{43})/2\right)} \tag{4}$$

$$\alpha_{EB} = \frac{N\mu_{13}\mu_{24} \exp(i(\varphi_2 - \varphi_1)\Lambda_c \exp(i(\varphi_c + \varphi))\widetilde{\rho}_{12}^{(0)})}{2\hbar K_b(\Delta_p - i(\gamma_{31} + \gamma_{43})/2)}$$
(5)

Furthermore,

$$K_b = \Delta_p - \frac{i\gamma_{31}}{2} - \frac{\Lambda_c^2}{4(\Delta_p - i(\gamma_{42} + \gamma_{43})/2)}$$
 (6)

$$K_e = \Delta_p - \frac{i(\gamma_{43} + \gamma_{42})}{2} - \frac{\Lambda_c^2}{4(\Delta_p - i(\gamma_{31})/2)}$$
 (7)

where, $\Lambda_c = |\Lambda_c| e^{i\varphi_c}$ and $B = \mu_0(M+H)$. The chiral coefficients for the electric polarization and magnetization, as well as the electric and magnetic susceptibilities, are represented as:

$$P = \frac{\xi_{EH}H}{c} + \epsilon_0 \chi_e^{(1)} E, M = \frac{\xi_{HE}H}{\mu_0 c} E + \chi_m^{(1)} H \qquad (8)$$

In order to compute the electric and magnetic susceptibilities and chiral coefficients, compare the polarization and magnetization as:

$$\chi_e = \frac{\alpha_{EB} + \mu_0(\alpha_{EB}\alpha_{BE} - \alpha_{EE}\alpha_{BB})}{\epsilon_0(1 - \mu_0\alpha_{BB})} \tag{9}$$



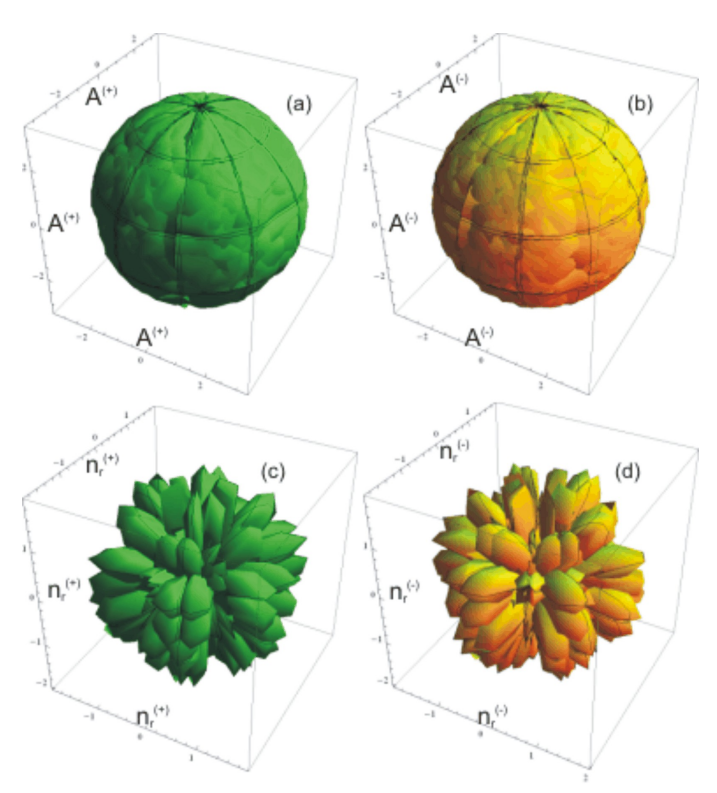


Figure 3. Absorptions and refractive indices of RCP and LCP beams in chiral medium such as $\varphi_c=\pi/3$, $\varphi=\pi/3$, $\varphi_1=\pi/2$, $\varphi_2=0$, $\gamma_{dc}=0.5\gamma$, $\gamma_{db}=0.5$, $\gamma_{ca}=0.02\gamma$, $|\Omega_c|=1.5\gamma$, $\Delta_p=1.5$, x=0.3.

$$\chi_m = \frac{\mu_0 \alpha_{BB}}{1 - \mu_0 \alpha_{BB}} \tag{10}$$

$$\xi_{EH} = \frac{c\mu_0 \alpha_{EB}}{1 - \mu_0 \alpha_{BB}} \tag{11}$$

$$\xi_{HE} = \frac{c\mu_0 \alpha_{BE}}{1 - \mu_0 \alpha_{BB}} \tag{12}$$

The incident light beam is birefringently split into left and right circularly polarized components by the chiral medium. The refractive indices of the LCP and RCP beams are $n_r^{(-)}$ and $n_r^{(+)}$, respectively. A formula for the birefringent light beam's complicated refractive indices looks like this:

$$n_r^{(\pm)} = \sqrt{(1 + \chi_e)(1 + \chi_m) - \frac{(\xi_{EH} + \xi_{HE})^2}{4}}$$
$$\pm i \frac{(\xi_{EH} - \xi_{HE})}{2}$$

Refractive indices come in a complex form, with the real and imaginary components corresponding to the velocity and amplitude attenuation, respectively. The index of a complex group expressed in terms of the refractive index and the detuning of the probing field

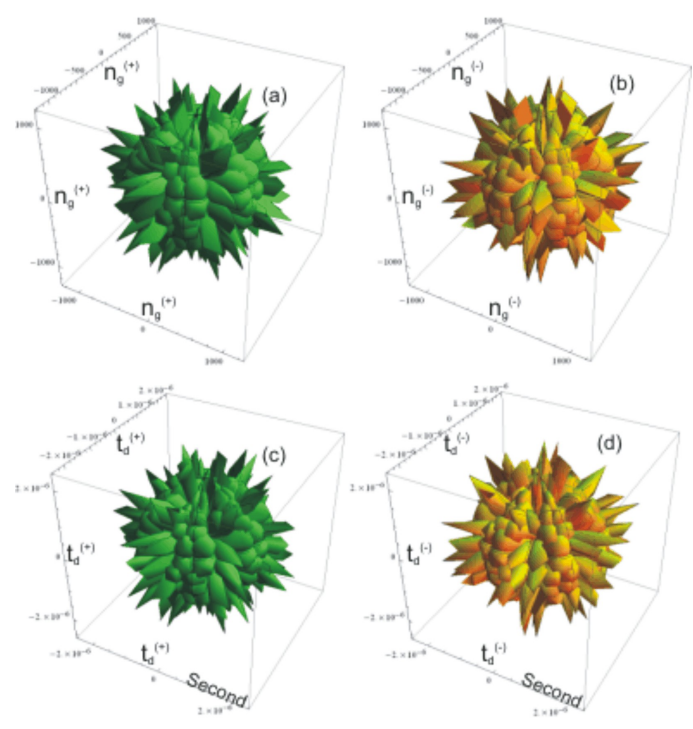


Figure 4. Group indices and delay times of RCP and LCP beams in chiral medium such as $\varphi_c = \$\gamma_{dc} = 0.5\gamma$, $\gamma_{db} = 0.5$, $\gamma_{ca} = 0.02\gamma$, $|\Omega_c| = 1.5\gamma$, $\Delta_p = 1.5$, x = 0.3.

is as follows:

$$n_g^{(\pm)} = Re(n_r^{(\pm)}) + \omega \frac{\partial Re(n_r^{(\pm)})}{\partial \Delta_p}$$
 (13)

In addition, $v_g^\pm=c/Re(n_g^{(\pm)})$ describes the relationship between the group velocity and the group index. and the medium's delay/advance time is represented as:

$$t_d = \frac{L}{c}(n_g^{(\pm)} - 1) \tag{14}$$

Where L is the distance traversed by the medium. Birefringent beams of left/right circular polarization display phase shifts as shown by the following expression:

$$\phi^{(\pm)} = k^{(\pm)}L = k_0 n_r^{(\pm)}L \tag{15}$$

The group phase shifts in left/right circularly polarized birefringent beam is given by

$$\phi_a^{(\pm)} = k^{(\pm)}L = k_0 n_a^{(\pm)}L \tag{16}$$

The fractional change group index, group delay time, and phase shift is written as:

$$F_{group-index} = \frac{n_g^{(+)} - n_g^{(-)}}{n_g^{(+)}}$$
 (17)

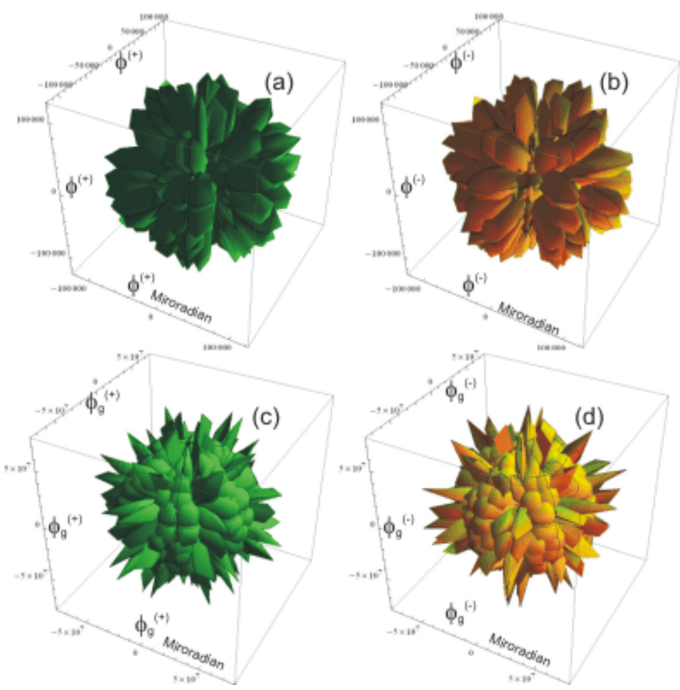


Figure 5. Phase shift and group phase shifts of RCP and LCP beams in a chiral medium such as $\varphi_c=\pi/3$, $\varphi=\pi/3$, $\varphi_1=\pi/2$, $\varphi_2=0$, $\gamma_{dc}=0.5\gamma$, $\gamma_{db}=0.5$, $\gamma_{ca}=0.02\gamma$, $|\Omega_c|=1.5\gamma$, $\Delta_p=1.5$, x=0.3.

$$F_{delay-time} = \frac{t_d^{(+)} - t_d^{(-)}}{t_d^{(+)}}$$
 (18)

$$F_{phase-shift} = \frac{\phi_g^{(+)} - \phi_g^{(-)}}{\phi_g^{(+)}}$$
 (19)

3 Results and discussions

In this work, we explore the spherical behavior of light beams with LCP and RCP in an atomic medium. The expected value of the γ scaling parameter is $2\pi\times5\times10^9Hz$. The angular frequency of intendment light is written by $\omega=1000\gamma$. The other parameters are $\mu_0=4\pi\times10^{-7}N/A^2,~c=3\times10^8m/s,~\epsilon_0=8.85\times10^{-12}C^2/Nm^2,~\hbar=1.0545\times10^{-34}Js,~N=5\times10^{12}atm/cm^3,~x=0.3,~2\pi c/\omega$ and $k_0=2\pi/\lambda$.

Absorptions of left and RCP light in a chiral material are plotted against x/λ and y/λ in Figure 3. Absorption of a circularly polarized beam from the right, as shown in Figure 3(a). The LCP beam is shown being absorbed in Figure 3(b). RCP and LCP beam absorption are spherical and symmetric about the center. $A_r^{(-)}$ and $A_r^{(+)}$ are the absorption coefficients for the left and right circularly polarized beams, respectively. The LCP beam is denoted by $A_r^{(-)}$ and the RCP beam by $A_r^{(+)}$. As can be seen in Figure 3(a) and Figure 3(b), the atomic

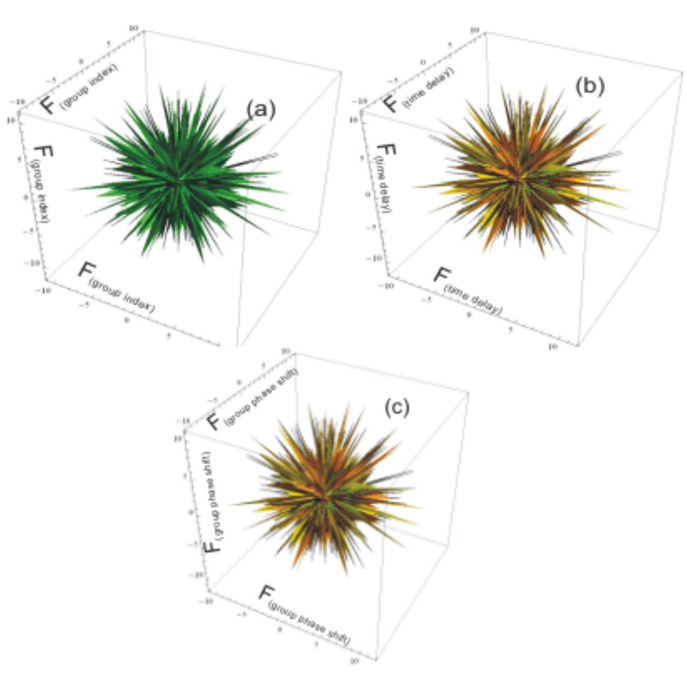


Figure 6. Fractional change in phase shifts and of RCP and LCP beams in a chiral medium such as $\varphi_c=\pi/3$, $\varphi=\pi/3$, $\varphi_1=\pi/2$, $\varphi_2=0$, $\gamma_{dc}=0.5\gamma$, $\gamma_{db}=0.5$, $\gamma_{ca}=0.02\gamma$, $|\Omega_c|=1.5\gamma$, $\Delta_p=1.5$, x=0.3.

medium has a spherical structure that absorbs both LCP and RCP beams. Circularly polarized beams can be either left or right, and both have refractive indices of $n_r^{(-)}$ or $n_r^{(+)}$. Here $n_r^{(-)}$ denotes the LCP beam, and $n_r^{(+)}$ denotes the RCP beam. Beams of LCP and RCP light have refractive indices that oscillate spherically as a function of position along the x/λ and y/λ axes. As may be seen in Figure 3(c) and Figure 3(d), the refractive index values of both beams are changed to ± 2 .

LCP and RCP in chiral mediums have their group index and delay time in the medium plotted against x/lambda and y/lambda in Figure 4. The group index shown in Figure 4(a) is for a right circularly polarized beam. Figure 4(b) shows the group index for a left circularly polarized beam. RCP and LCP beams share the same spherical and rotationally symmetric about the origin group index. Both the left and right circularly polarized beams have group indices of $n_g^{(-)}$ and $n_g^{(+)}$, respectively. The LCP beam is denoted by $n_g^{(-)}$ and the RCP beam by $n_g^{(+)}$. There are only two possible large values for the group index: $n_g^{(+)} = \pm 1000$ and $n_g^{(-)} = \pm 1000$. Group velocities of $v_g^{(+)} = \pm c/1000$ and $v_g^{(-)} = \pm c/1000$, respectively, are thus attained.Propagation of the LEC and RCP beam is subluminal when the group velocity is $v_g^{(\pm)} = +c/1000$, and it is superluminal when the group velocity is



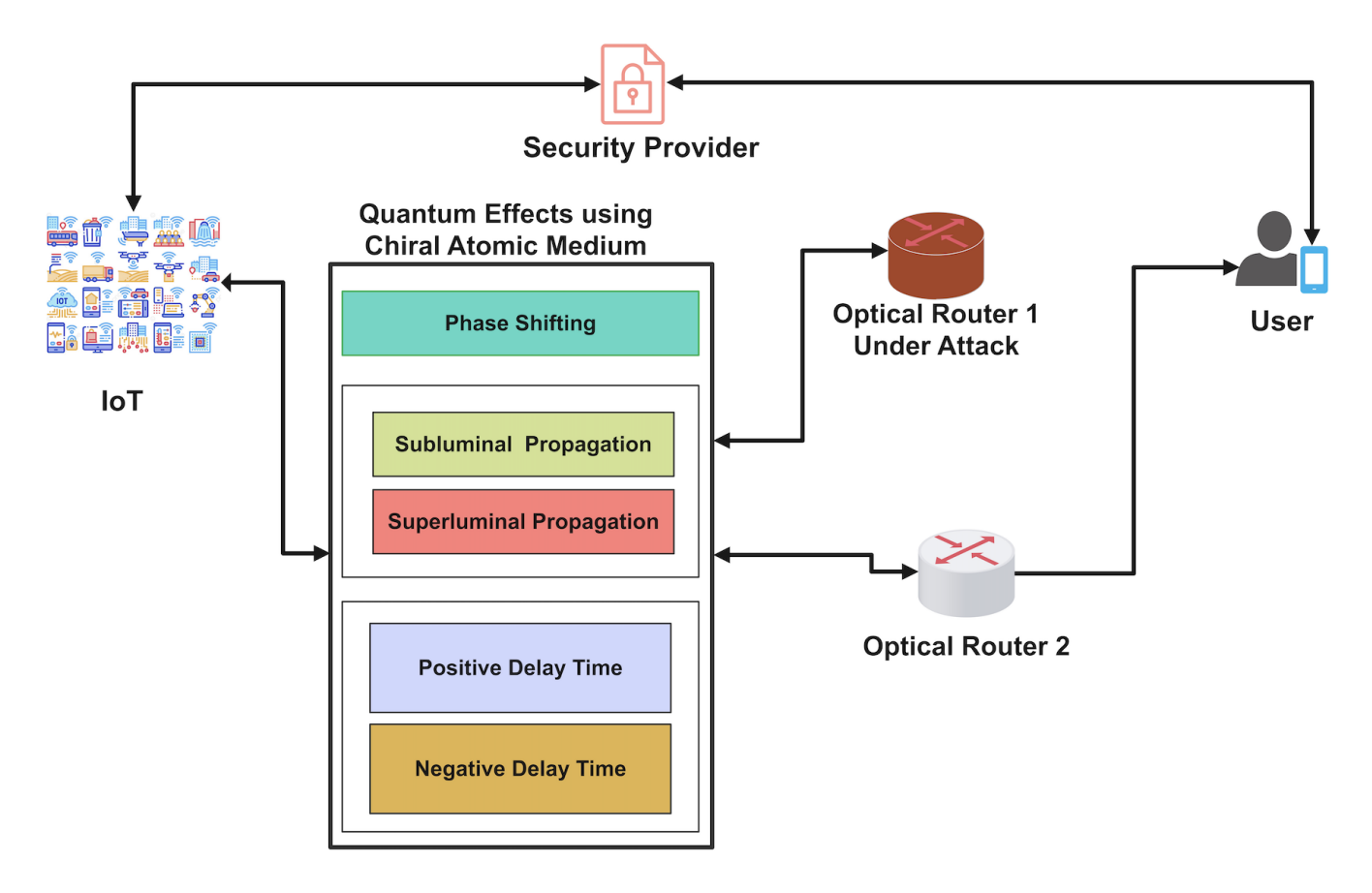


Figure 7. Use cases of the proposed scheme.

 $v_q^{(\pm)} = -c/1000$. As can be seen in Figure 4(a) and Figure 4(b), the group index of both the LCP and RCP beams in the atomic medium is spherical and symmetric at the origin of the coordinates. Also, the delay time is symmetrical about the coordinate origin, making it a sphere. For both LECP and RCP beams, the maximum delay time in a chiral medium is $\pm 2\mu s$. The positive value indicates that the time it takes for the pulse to travel through the medium at length L is longer than the time it takes for the pulse to travel through the vacuum at length L, as indicated by the expression $t_m > t_0$, where $t_m > t_0$, where $t_m = L/v_g$ and $t_v = L/c$. When delay has a negative value, it means that the time it takes for the pulse to travel L in the medium is less than the time it takes to travel L in the vacuum, as in the case where $t_m < t_0$. According to Figure 4(c) and Figure 4(d), subluminality is associated with $t_m > t_0$, while superluminality is associated with $t_m < t_0$.

Phase shifts of LECP and RCP beams, as well as group phase shifts for LCP and RCP beams in a chiral medium, are plotted against x/λ and y/λ in Figure 5. Phase shift $\phi^{(+)}$ in the right circularly polarized beam is shown in Figure 5(a), while phase shift $\phi^{(-)}$ is shown in Figure 5(b). Figure 5(c) depicts the phase shift

in the RCP beam group $\phi_g^{(+)}$, whereas Figure 5(d) depicts the phase shift in the LCP beam group $\phi_g^{(-)}$. As can be seen in Figure 5(a) and Figure 5(b), the phase shifts in LCP and RCP beams are spherically symmetric at the origin of x,y,z=0 and range from 0 micro-radian to $\pm 10^5$ micro-radian. As can be seen in Figure 5(c) and Figure 5(d), the group phase shifts in the LCP and RCP beams range from zero micro-radian to $\pm 10^7$ micro-radian and are spherically symmetric about the origin of x,y,z=0.

The Figures for the fractional change in the group indices, delay time, and phase shifts of LCP and RCP beams in chiral media vs x/lambda and y/lambda are shown in Figure 6. These Figure 6 are traced against x/lambda and y/lambda, respectively. Around the point where x, y, and z equal zero, the fractional change in group indices, group delay time, and group phase shifts is spherically symmetric. In a strong spherical oscillating function of x/lambda and y/lambda, the value of the fractional change in group indices, as well as the group delay time and the group phase, varies around the origin. As can be seen in Figure 6(a), Figure 6(b), and Figure 6(c), the maximum fractional change in group indices, group delay time, and group

phase shifts is equal to pm10 = pm1000

4 Use case for the proposed scheme in IoT and sensors

In the current work, we investigated the subluminal/superluminal light propagation. In superluminal cases, the data is transferred faster than the conventional ones, and the efficiency of IoT devices is enhanced. We also investigated the time delay, whose negative value enhances the storage capacity of tiny IoT devices. Furthermore, we also investigated the phase shift. This quantum effect is used in cloaking devices that enhance the security of IoT and minimize data losses.

All these effects are also investigated by Karim et al. [6] They also presented the deployment of their work in IoT. The achiral atomic medium was used in their work, having certain shortcomings. We used the chiral atomic medium, which has certain advantages.

A light beam is split into two parts as it passes through a chiral medium; these two components are referred to as LCP and RCP, respectively. Because of this property, the capacity of quantum sensors to make decisions is improved thanks to selective absorption. In addition to this, the chiral medium that we have described is able to control the polarization of light that is transmitted through it. Due to this occurrence, it is possible to implement effective optical routing, as shown in Figure 7, which depicts EM waves being redirected from faulty routers to others that are operating normally. Additionally, it improves phase shifting, which in turn helps improve the security of IoT.

5 Conclusion

The quantum-based models are used to improve Internet of Things (IoT) ecosystems' security, efficiency, storage capacity, and data transmission speed. These models investigate the proposed goals' significant quantum effects like subluminality/superluminality, time delay, and phase shift. Mostly, these models use achiral atomic media that deal with the light beam in a straight path and fail to provide the most needed properties of efficient decision-making, optical routing, control of polarization, and enhanced security. Keeping in mind the aforementioned shortcomings, The propagation of spherical behaviours of light beams in a chiral medium is controlled and modified with control fields and system parameters. The light beam is split into left and right circularly polarized beams in

the chiral medium to provide efficient decision-making and optical routing for quantum-based IoT devices. The left and right circularly polarization beams are related to corresponding absorption, refractive indices, group indices, and phase shifts in the medium, show spherical as well as symmetrical behaviour along the coordinates axis about the origin in the medium. The maximum values of group indices are varied to $n_g^{(\pm)}=\pm 1000$. This corresponds to $v_g^{(\pm)}=\pm c/1000$ group velocities. The positive value of group velocity $v_q^{(\pm)} = +c/1000$ shows subluminal propagation of LCP and RCP beams and the negative value of velocity $v_q^{(\pm)} = -c/1000$ indicates superluminal propagation which enhances the data transfer speed in IoT. The maximum phase shifts in RCP and LCP beams are measured to $\pm 10^5$ Micro-radian and group phase shifts are measured to $\pm 10^5$ micro-radian, used to enhance the security of IoT as well as minimize losses. The maximum fractional change is measured to $\pm 10 = \pm 1000\%$ in group indices, group delay time, and group phase shifts of LCP and RCP beams in a chiral medium.

Data Availability Statement

Data will be made available on request.

Funding

This work was supported without any funding.

Conflicts of Interest

The authors declare no conflicts of interest.

Ethical Approval and Consent to Participate

Not applicable.

References

- [1] Schöffel, M., Lauer, F., Rheinländer, C. C., & Wehn, N. (2022). Secure IoT in the era of quantum computers—Where are the bottlenecks?. *Sensors*, 22(7), 2484. [CrossRef]
- [2] Gautam, S., Solanki, S., Sharma, S. K., Chatzinotas, S., & Ottersten, B. (2022). Boosting quantum battery-based IoT gadgets via RF-enabled energy harvesting. *Sensors*, 22(14), 5385. [CrossRef]
- [3] Arif, S. M., Bacha, B. A., Ullah, S. S., Hussain, S., & Haneef, M. (2022). Tunable control of internet of things information hacking by application of the



- induced chiral atomic medium. *Soft Computing*, 26(20), 10643-10650. [CrossRef]
- [4] Bashir, A. I. (2023). Quantum coherence-assisted secure communication of internet of things information via Landau-quantized graphene. *Optical and Quantum Electronics*, 55(11), 983. [CrossRef]
- [5] Kitano, M., Nakanishi, T., & Sugiyama, K. (2003). Negative group delay and superluminal propagation: An electronic circuit approach. *IEEE Journal of selected Topics in Quantum electronics*, 9(1), 43-51. [CrossRef]
- [6] Karim, F., Haneef, M., Sajid Ullah, S., Alsafyani, M., Alroobaea, R., Algarni, S., & Hussain, S. (2023). Manipulation speed of light and giant phase shifting: a new quantum-based model for improving efficiency and security of internet of things. *Optical and Quantum Electronics*, 55(9), 796. [CrossRef]
- [7] Mun, J., Kim, M., Yang, Y., Badloe, T., Ni, J., Chen, Y., ... & Rho, J. (2020). Electromagnetic chirality: from fundamentals to nontraditional chiroptical phenomena. *Light: Science & Applications*, 9(1), 139. [CrossRef]
- [8] Hannam, K., Powell, D. A., Shadrivov, I. V., & Kivshar, Y. S. (2014). Broadband chiral metamaterials with large optical activity. *Physical Review B*, 89(12), 125105. [CrossRef]
- [9] Arif, S. M., Bacha, B. A., Wahid, U., Ullah, A., & Haneef, M. (2021). Tunnelling based birefringent phase sensitivity through dynamic chiral medium. *Physica Scripta*, *96*(3), 035106. [CrossRef]
- [10] Arif, S. M., Bacha, B. A., Wahid, U., Haneef, M., & Ullah, A. (2021). Tunable subluminal to superluminal propagation via spatio-temporal solitons by application of Laguerre fields intensities. *Physics Letters A*, 388, 127041. [CrossRef]



Saddam Hussain is working with the School of Digital Science, Universiti Brunei Darussalam, Gadong, Brunei. He has published several papers in well-reputed journals, including IEEE, JISA, Elsevier, Cluster Computing, Computer Communication, IoTJ, and Electronics. He is serving as a reviewer in reputed journals including IEEE Access, International Journal of Wireless Information Networks, Scientific Journal of Electrical

Computer and Informatics Engineering, and CMC. His research interests include cryptography, network security, Wireless Sensor Networking (WSN), Information-Centric Networking (ICN), Named Data Networking (NDN), smart grids, Internet of Things (IoT), IIoT, quantum computing, cloud computing, and edge computing.



Syed Sajid Ullah received his Master's degree in computer science from Hazara University, Pakistan, and earned his Ph.D. through a joint program between Villanova University, USA, and the University of Agder, Norway. He is currently a researcher at the Department of Information and Communication Technology at the University of Agder (UiA), Grimstad, Norway. Soon, he will be joining the University of Sydney as an Assistant Professor. He is an

active member of the academic community, having authored over 100 publications in high-impact journals. He serves as an editor for IEEE Access, PeerJ Computer Science, Sensors, and Scientific Reports and is on the editorial boards of several reputable journals. He also contributes regularly as a reviewer for more than 30 esteemed publications. His research focuses on cryptography, blockchain, access control, post-quantum cryptography, network security, information-centric networking, named data networking, and the Internet of Things (IoT). Additionally, he plays a key role in the NIST-funded project on quantum cryptography and named data networking. (Email: sajidullah718@gmail.com)